

Synthesis, Characterization, and Thermal Properties of Fluoropyridyl-Functionalized Siloxanes of Diverse Polymeric Architectures

Kevin A. Stewart, Dylan Shuster, Maria Leising, Isaac Coolidge, Erica Lee, Charles Stevens, Andrew J. Peloquin, Daniel Kure, Abby R. Jennings,* and Scott T. Iacono*

Cite This: <https://doi.org/10.1021/acs.macromol.1c00333>

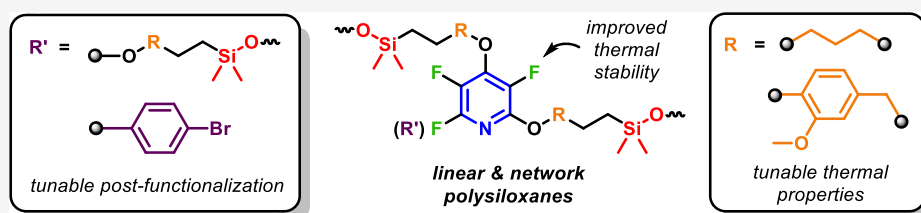
Read Online

ACCESS |

Metrics & More

Article Recommendations

Supporting Information



ABSTRACT: High-temperature linear fluoropyridyl silicone-based oils and network elastomers were prepared via hydrosilylation with multifunctional perfluoropyridine (PFP)-based monomers possessing terminally reactive alkenes. Monomers with varying degrees of functionalization were prepared in a scalable manner and in high purity via the facile, regio-selective, nucleophilic aromatic substitution (S_NAr) of PFP in good isolated yields. These multi-reactive monomers were polymerized via Pt-catalyzed hydrosilylation with hydride-terminated polydimethylsiloxanes (H-PDMSs) possessing varying degrees of polymerization and cross-linked with the highly functionalized octadimethylhydrosilyl cubic siloxane. These resulting polymers of varying architecture possessed exceptional thermal stability with no onset of degradation up to 430 °C and char yields as high as 62%, under inert pyrolysis conditions when modified with cubic siloxane. Furthermore, by nature of the aliphatic or aromatic content, programmable glass transition temperatures were achieved from these elastomeric materials. Finally, the linear 3,5,6-fluoropyridine PDMS systems demonstrated the ability to undergo regio-controlled post-functionalization via S_NAr with 4-bromophenol, allowing access to silicone oils with potentially tailorable properties for desired applications.

INTRODUCTION

High-performance materials, heavily composed of elastomers and thermosetting resins, serve a critical role in a variety of applications, especially within the fields of commercial and military aerospace technologies.¹ One such application that high-performance elastomers have greatly underpinned is for heat-shielding materials (HSMs) in rocket motor casings.² Material reliability in HSMs focuses strongly on a wide range of service temperatures and high carbonaceous char following degradation. Consequently, typical long-term low-temperature (often cryogenic) storage must not jeopardize the material's performance at ultimately elevated operational temperatures, whereupon eventual pyrolysis ideally leaves sufficient levels of a sacrificial, protective char. Thus, polymer candidates should possess sufficiently low glass transition temperatures (T_g 's) so that the material remains flexible at sub-freezing temperatures but boasts thermal/thermo-oxidative dependability at or above 300–350 °C.³

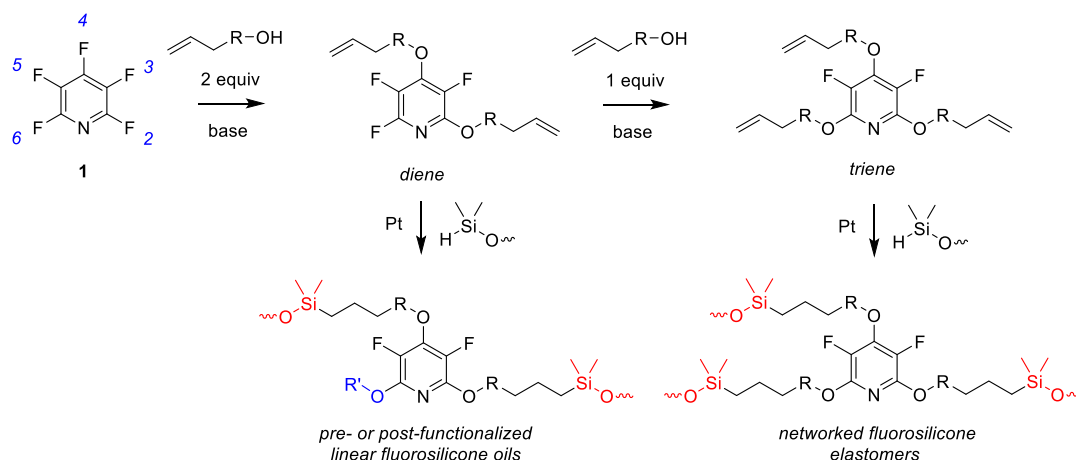
Due to the markedly high bond strength and flexibility of the silicon–oxygen bond, siloxane-containing polymers have unprecedented thermo-oxidative stability and low T_g 's.⁴ Therefore, silicone elastomers are attractive materials for

high-performance functionality. Additionally, these materials can be accessed via facile procedures, including metal-free azide–alkyne and thiol–ene click chemistries.^{5–7} However, one of the most common and rapid methods remains the platinum-catalyzed hydrosilylation reaction. The incorporation of siloxane segments into polymers provides a number of enhanced properties to these materials, such as low surface energy, chemical resistance, low T_g , resistance to impact damage or fracture, and thermal stability.^{8–12} Common siloxane additives include polydimethylsiloxane (PDMS) and polyhedral oligomeric silsequioxane (POSS) macromers, the latter receiving substantial recognition in recent years for its diverse features. The robust POSS cage architecture is an attractive platform due to its high degree of tunability and ease of incorporation, demonstrably augmenting their use in

Received: February 11, 2021

Revised: March 19, 2021

Scheme 1. Accessing Pyridyl-Functionalized Fluorosilicones of Linear and Networked Architecture by Regio-Controlled Functionalization of PFP (1) with Alcohols Possessing Terminal Alkenes that Undergo Hydrosilylation with H-PDMS^a



^aThe resulting linear polymers (via diene monomer) afford viscous oils that can be pre- or post-functionalized and networks (via triene monomer) that have programmable elasticity.

thermoplastic elastomers, polymer composites, and reprocessable thermosetting networks (vitrimers).^{13–21} Hence, the incorporation of POSS components is a distinct and expedient option for the fabrication of novel high-performance thermosets and elastomers.

A subsidiary of siloxane materials is fluorosilicone rubbers/resins (FSRs). FSRs possess qualities that are enhanced compared to traditional silicones such as hydrophobicity, chemical and thermal robustness, and resistance to weathering.^{22–24} However, FSR manufacturing and, therefore, all-purpose use, is often hampered by the high cost of production. Additionally, FSRs are generally limited to a narrow monomer scope—typically composed of fluoroalkyl substituents. Nevertheless, FSRs offer a route to materials that can withstand the harsh conditions required for high-performance applications by combining the exceptional characteristics of silicones with those of fluoropolymers.

Perfluoroaromatics (PFAR's) have proven to be highly advantageous synthetic building blocks for diversifying polymeric materials, attributable to predictable nucleophilic substitution patterns and a range of nucleophile tolerability.²⁵ Additionally, the high fluorine content in conjunction with aromaticity imparted to polymers derived from PFAR's endows these materials with exceptional thermal stability and processability.^{26,27} Of the many PFAR's, perfluoropyridine (PFP) has proven to be an auspicious scaffold for fluoropolymer design, owing to its predictable and discrete regio-selective substitution pattern at the 2-, 4-, and 6-positions on the ring, its predilection for chemo-selective nucleophilic aromatic substitution, and its wide scope of nucleophile permissibility.^{28–31} These properties permit facile incorporation of PFP into novel polymer architectures, allowing for diverse and tailorable material properties.^{32–34} As shown in Scheme 1, PFP (1) offers unique opportunities to design linear (via diene monomers) and network (from triene monomers) polymers in addition to tailoring pre-functionalized monomers and post-polymerization modification. The research herein describes these applications of the modular PFP scaffold for use in semi-fluorinated silicone oils and elastomers utilizing hydrosilylation chemistry. The thermal properties of the resultant polymers and elastomers offer an alternative route

to a more diverse pool of highly tailorable, high-performance fluorosilicone materials.

EXPERIMENTAL SECTION

Methods. HPLC-grade tetrahydrofuran was dried and deoxygenated by passage through a Pure-Solv solvent purification system equipped with Cu/Al columns from Innovative Technologies. Anhydrous dimethylformamide was further dried by storage over anhydrous magnesium sulfate under a nitrogen atmosphere. Glassware and syringes were flamed-dried and allowed to cool in a desiccator prior to use. Syringes fastened with syringe needles were flushed with nitrogen prior to use. All reactions and solvent transfers were carried out under an atmosphere of nitrogen.

Materials. Chemicals and solvents, which were of reagent grade, were purchased through commercial suppliers and used as received, unless specifically noted. The synthesis of 5, 7, and 8 was carried out from previously published work.^{31,34}

Instrumentation. ¹H, ¹³C, and ¹⁹F NMR spectra were recorded on a JEOL 500 MHz spectrometer. Chemical shifts were reported in parts per million (ppm), and the residual solvent peak was used as an internal reference: proton (chloroform δ 7.26), carbon (chloroform, C{D} triplet, δ 77.0 ppm), and fluorine (CFCl₃, δ 0.00) was used as a reference. Data are reported as follows: chemical shift, multiplicity (s = singlet, m = multiplet), coupling constants (Hz), and integration.

Gas chromatography–mass spectrometry (GC–MS) analyses were performed on an Agilent 7890 gas chromatograph coupled to an Agilent 5975C electron impact mass spectrometer with a temperature gradient of 80–250 °C at 15 °C min⁻¹ after an initial 2 min temperature hold at 80 °C.

Differential scanning calorimetry (DSC) analyses were performed on a TA Q20 or Q200 DSC utilizing aluminum hermetic pans. The analyses were carried out using a 5 °C min⁻¹ temperature gradient under nitrogen. Thermogravimetric analyses (TGAs) were performed on a TA Q500 utilizing platinum pans at a 10 °C min⁻¹ temperature gradient under argon.

Gel permeation chromatography (GPC) data in tetrahydrofuran (HPLC-grade) were collected using polystyrene as a standard (Polymer Labs Easical PS-2) using a Agilent PL-GPC 220 System, whereby samples were eluted in series through Agilent PLgel Mixed-D and Mixed-E columns at 35 °C.

Synthesis of 2,3,5-Trifluoro-4,6-bis(pent-4-en-1-yloxy)pyridine (2). 4-Penten-1-ol (2.5 equiv, 7.14 mL, 165.3 mmol), PFP (1 equiv, 7.28 mL, 66.37 mmol), and cesium carbonate (4 equiv, 86.5 g, 265 mmol) were added to acetonitrile (500 mL) and allowed to stir at room temperature for 3 d. The reaction is typically

monitored by GC–MS until 100% conversion of the desired product is observed. The reaction is then vacuum-filtered and concentrated using rotary evaporation. The crude mixture is then reconstituted with diethyl ether (250 mL), and then, saturated ammonium chloride (250 mL) is added in order to perform liquid–liquid extraction. The saturated ammonium chloride is extracted with diethyl ether (3 × 50 mL), and the combined diethyl ether fractions are washed with deionized water (250 mL), saturated brine (250 mL) and dried with magnesium sulfate. The crude reaction mixture is then vacuum-filtered, dried using rotary evaporation, and vacuum-filtered through a silica plug (100 g) using 95:5 (hexanes/ethyl acetate) as the mobile phase. The filtrate was concentrated by rotary evaporation and dried under high vacuum, affording a clear, colorless oil (17.2 g, 86%). ¹H NMR (CDCl₃, 500 MHz): δ 5.83–5.80 (m, 2H), 5.07–4.99 (m, 4H), 4.41–4.26 (m, 4H), 2.23–2.19 (m, 4H), 1.89–1.85 (m, 4H); ¹⁹F NMR (CDCl₃, 471 MHz): δ –93.78 (s, 1F), –160.0 (s, 1F), –166.9 (s, 1F); GC–EIMS (70 eV) *m/z* (% relative intensity) 301 (M⁺, 5), 233 (30), 205 (25), 165 (35), 68 (85), 53 (5), 41 (100).

Synthesis of 2-(4-Bromophenoxy)-3,5-difluoro-4,6-bis(pent-4-en-1-yloxy)pyridine (3). Cesium carbonate (7.56 g, 23.2 mmol), 2,3,5-trifluoro-4,6-bis(pent-4-en-1-yloxy)pyridine (2) (3.49 g, 11.6 mmol), and 4-bromophenol (2.05 g, 11.8 mmol) were added in dimethylformamide (50 mL) and allowed to stir for 24 h at 65 °C. The reaction is typically monitored by ¹⁹F until 100% conversion of the desired product is observed. The solution was vacuum-filtered and flushed with chloroform (100 mL). The filtrate was added to a separatory funnel with saturated ammonium chloride (100 mL). The aqueous layer was extracted with chloroform (3 × 50 mL), and the combined organic fractions were washed with saturated brine (5 × 50 mL), dried with magnesium sulfate, vacuum-filtered, concentrated using rotary evaporation, and dried under high vacuum, affording a pale yellow oil (3.03 g, 70%). ¹H NMR (CDCl₃, 500 MHz): δ 7.45–7.43 (d, 2H), 6.99–6.96 (m, 2H), 5.82–5.73 (m, 2H), 5.01–4.96 (m, 4H), 4.40–4.38 (s, 2H), 4.08–4.05 (s, 2H), 2.26–2.23 (m, 4H), 2.08–2.06 (m, 4H), 1.90–1.87 (m, 4H), 1.75–1.71 (m, 4H); ¹³C NMR (100 MHz): δ 137.6, 137.4, 122.0, 115.7, 115.2, 73.5, 66.4, 30.1, 29.7, 29.1, 29.7; ¹⁹F NMR (CDCl₃, 471 MHz): δ –161.8 (s, 1H), 163.2 (s, 1H); GC–EIMS (70 eV) *m/z* (% relative intensity) 455, 453 (M⁺, 20, 20), 319, 317 (80, 80), 238 (80), 214 (30), 69 (100).

Synthesis of 2,4-Bis(4-allyl-2-methoxyphenoxy)-3,5,6-trifluoropyridine (4). Cesium carbonate (6.05 g, 18.6 mmol), PFP (0.912 mL, 8.31 mmol), and eugenol (2.641 mL, 17.1 mmol) were added in dimethylformamide (100 mL) and allowed to stir for 24 h at room temperature. The reaction is typically monitored by ¹⁹F until 100% conversion of the desired product is observed. The solution was vacuum-filtered and flushed with diethyl ether (100 mL). The filtrate was added to a separatory funnel with saturated ammonium chloride (100 mL). The aqueous layer was extracted with diethyl ether (3 × 50 mL), and the combined organic fractions were washed with saturated brine (5 × 50 mL), dried with magnesium sulfate, vacuum-filtered, concentrated using rotary evaporation, and dried under high vacuum, affording an off-white, waxy solid (1.53 g, 39%). ¹H NMR (CDCl₃, 500 MHz): δ 7.05–7.00 (m, 2H), 6.80–6.73 (m, 4H), 6.00–6.85 (m, 2H), 5.13–5.07 (m, 4H), 3.83 (s, 3H), 3.74 (s, 3H), 3.39–3.67 (m, 4H); ¹³C NMR (126 MHz): δ 151.2, 150.0, 143.5, 139.7, 138.8, 138.1, 137.1, 137.0, 122.5, 120.9, 120.7, 118.8, 116.8, 113.2, 113.1, 56.01, 55.9, 40.1, 40.0; ¹⁹F NMR (CDCl₃, 471 MHz): δ –91.2 (s, 1F), –156.0 (s, 1H), –162.7 (s, 1H); GC–EIMS (70 eV) *m/z* (% relative intensity) 457 (M⁺, 15), 426 (10), 255 (10), 281 (50), 207 (100), 147 (30), 131 (20), 115 (20), 91 (30), 73 (80).

Synthesis of 2,6-Bis(4-allyl-2-methoxyphenoxy)-3,5-difluoro-4-phenylpyridine (6). Cesium carbonate (3.80 g, 11.6 mmol), 2,3,5,6-tetrafluoro-4-phenylpyridine (5) (1.32 g, 5.8 mmol), eugenol (1.90 g, 11.6 mmol), and dimethylformamide (20 mL) were mixed and allowed to stir for 24 h at room temperature. The reaction is typically monitored by ¹⁹F until 100% conversion of the desired product is observed. The solution was vacuum-filtered and flushed with diethyl ether (50 mL). The filtrate was added to a separatory funnel with saturated brine (100 mL). The aqueous layer was

extracted with diethyl ether (3 × 25 mL) and the combined organic fractions were washed with saturated brine (5 × 25 mL), dried with magnesium sulfate, vacuum-filtered, concentrated using rotary evaporation, and dried under high vacuum, affording an off-white, waxy semi-crystalline solid (2.60 g, 77%). X-ray diffraction-quality single crystals were harvested from the waxy semi-crystalline solid after allowing one month of undisturbed settling in a round-bottom flask at ambient temperature (~20 °C). ¹H NMR (CDCl₃, 500 MHz): δ 7.58–7.46 (m, 6H), 6.88–7.86 (m, 2H), 6.60–6.56 (s, 3H), 5.98–5.92 (m, 2H), 5.11–5.08 (m, 4H), 3.50 (br s, 6H), 3.34–3.25 (m, 4H), 5.96–5.88 (m, 2H), 5.07–5.05 (t, 4H), 3.53 (s, 6H), 3.30 (d, *J* = 6.59 Hz, 4H), 1.5 (s, 9H); ¹³C NMR (CDCl₃, 126 MHz): δ 151.6, 144.3, 144.2, 140.4, 139.6, 137.6, 137.5, 137.4, 130.1, 129.9, 129.5, 128.6, 127.9, 122.3, 120.3, 116.0, 112.5, 55.7, 40.7; ¹⁹F NMR (CDCl₃, 471 MHz): δ –150 (s, 2F); GC–EIMS (70 eV) *m/z* (% relative intensity) 515 (M⁺, 20), 454 (25), 281 (50), 207 (100), 147 (20), 73 (50).

Synthesis of poly2. H-PDMS (1000 g mol⁻¹ avg molecular weight, 500 mg, 0.5 mmol) was added to 2 (150.3 mg, 0.5 mmol), and then, 1 drop of Pt catalyst (5 wt % platinum divinyltetramethyldisiloxane complex in xylene) was added. The solution was stirred at room temperature for 24 h. The product was used without further purification, affording a brown liquid.

¹H NMR (CDCl₃, 500 MHz): δ 4.50–4.48 (m), 4.39–4.73 (m), 4.27–4.24 (m), 2.23–2.20 (m), 1.78–1.76 (m), 1.54–1.38 (m), 0.57–0.54 (m), 0.20–0.00 (m); ¹⁹F NMR (CDCl₃, 471 MHz): δ –90.8 (br s), –93.9 (br s), –159.1 (br s), –159.9 (br s), –167.137 (br s).

Synthesis of poly3 from Pre-modified Monomer 3. H-PDMS (1000 g mol⁻¹ avg molecular weight, 500 mg, 0.5 mmol) was added to 3 (227 mg, 0.5 mmol), and then, 1 drop of Pt catalyst (5 wt % platinum divinyltetramethyldisiloxane complex in xylene) was added. The solution was stirred at room temperature for 24 h. The product was used without further purification, affording a brown liquid.

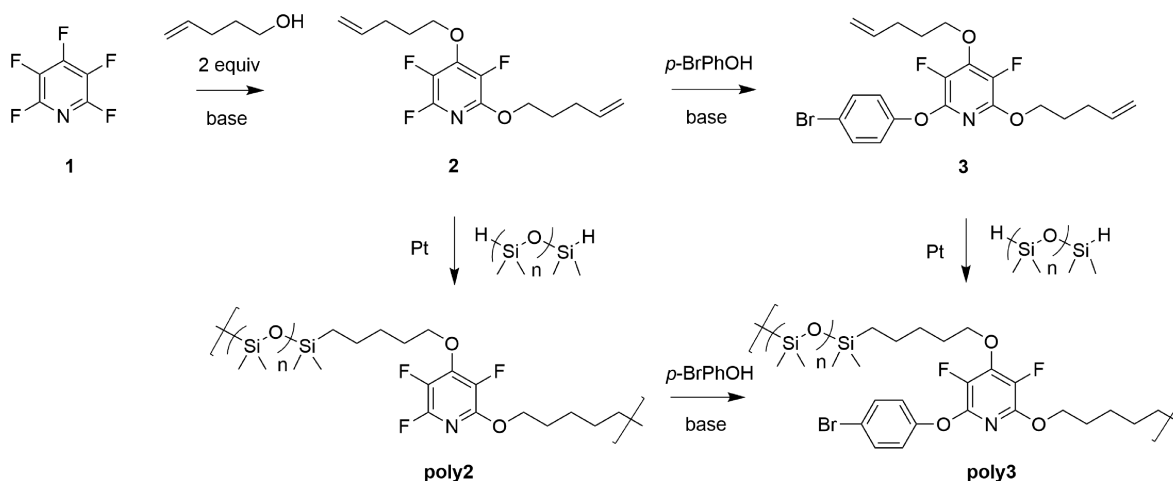
¹H NMR (CDCl₃, 500 MHz): δ 7.44–7.43 (m), 6.98–6.59 (m), 4.37–4.34 (m), 4.06–4.02 (m), 2.30–2.25 (m), 1.78–1.30 (m), 0.56–0.53 (m), 0.15–0.00 (m); ¹⁹F NMR (CDCl₃, 471 MHz): δ –161.7 to –161.3 (m), –163.2 (br, s).

Synthesis of poly3 from Post-modification of poly2. 4-Bromophenol (1.1 mmol), cesium carbonate (3 mmol), and poly2 (1 mmol) dissolved in *d*₇-dimethylformamide were added in an NMR tube and placed in a sonication bath at 60 °C for 3–5 d until conversion to the desired post-modified polymer was complete. ¹⁹F NMR (CDCl₃, 471 MHz): δ –159.0 to –161.3 (br, s), 168.8–169.9 (br, s).

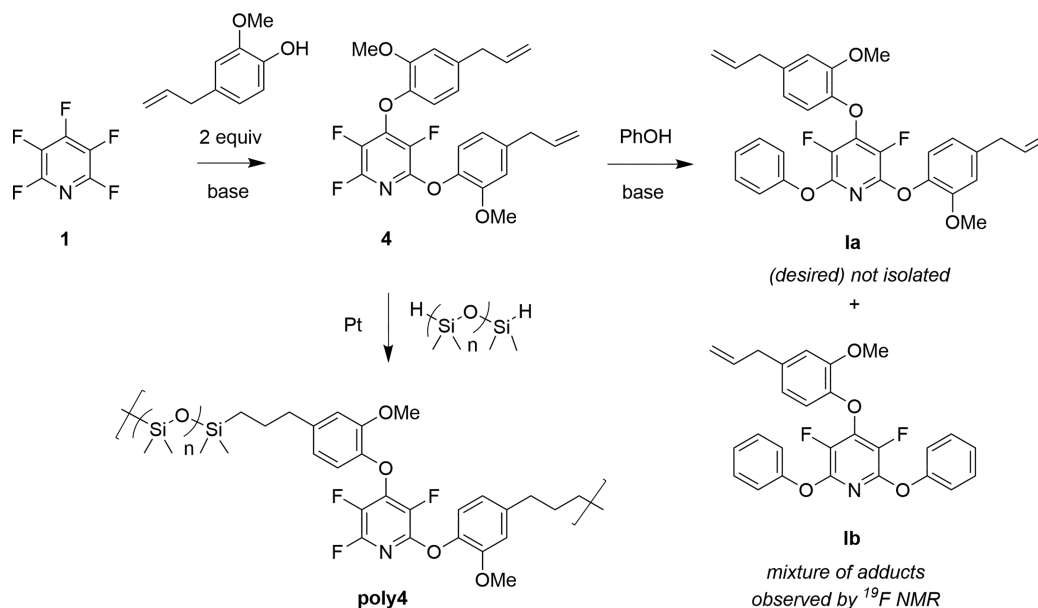
Synthesis of poly4. H-PDMS (1000 g mol⁻¹ avg molecular weight, 500 mg, 0.5 mmol) was added to 4 (229 mg, 0.5 mmol) in toluene (0.83 mL). The solution was sonicated, and then, 1 drop of Karstedt's catalyst (5 wt % platinum divinyltetramethyldisiloxane complex in xylene) was added and the solution was stirred at room temperature for 24 h. The solution was dried under high vacuum at 80 °C, affording a viscous brown liquid. ¹H NMR (CDCl₃, 500 MHz): δ 7.02–6.98 (m), 6.78–6.15 (m), 3.83 (br s), 3.75 (br s), 2.64–2.59 (m), 1.90–1.85 (m), 1.69–1.54 (m), 0.62–0.57 (m), 0.40–0.00 (m); ¹⁹F NMR (CDCl₃, 471 MHz): δ –91.4 (br s), –156.0 (br s), –162.7 (br s).

Synthesis of poly6. H-PDMS (1000 g mol⁻¹ avg molecular weight, 500 mg, 0.5 mmol) was added to 6 (256 mg, 0.5 mmol) in toluene (0.83 mL). The solution was sonicated, and then, 1 drop of Pt catalyst (5 wt % platinum divinyltetramethyldisiloxane complex in xylene) was added and the solution was stirred at room temperature for 24 h. The solution was dried under high vacuum at 80 °C, affording a viscous brown liquid. ¹H NMR (CDCl₃, 500 MHz): δ 7.57–7.47 (m), 6.85–6.83 (m), 6.58–6.54 (m), 3.55 (br s), 2.56–2.53 (m), 1.89–1.80 (m), 1.63–1.53 (m), 0.60–0.57 (m), 0.21–0 (m); ¹⁹F NMR (CDCl₃, 471 MHz): δ –147.5–149.9 (m).

General Synthesis of Networks net7a–7d and net8a–8d. To compound 7 or 8 (1.0 mmol) was added H-PDMS (1.0 mmol). The vial was then vortexed at room temperature for 1 min; 1 drop of Pt catalyst (5 wt % platinum divinyltetramethyldisiloxane complex in

Scheme 2. Synthesis of 2 and Subsequent Polymerization with H-PDMS to poly2^a

^aPre-installation of 2 with 4-bromophenol produced 3 and subsequently poly3, which can also be prepared from the post-functionalization of poly2.

Scheme 3. Synthesis of 4 and Subsequent Polymerization with H-PDMS to poly4^a

^aAttempts to pre-install 4 with phenol failed to produce the desired product Ia but afforded a mixture of adducts, primarily of Ib.

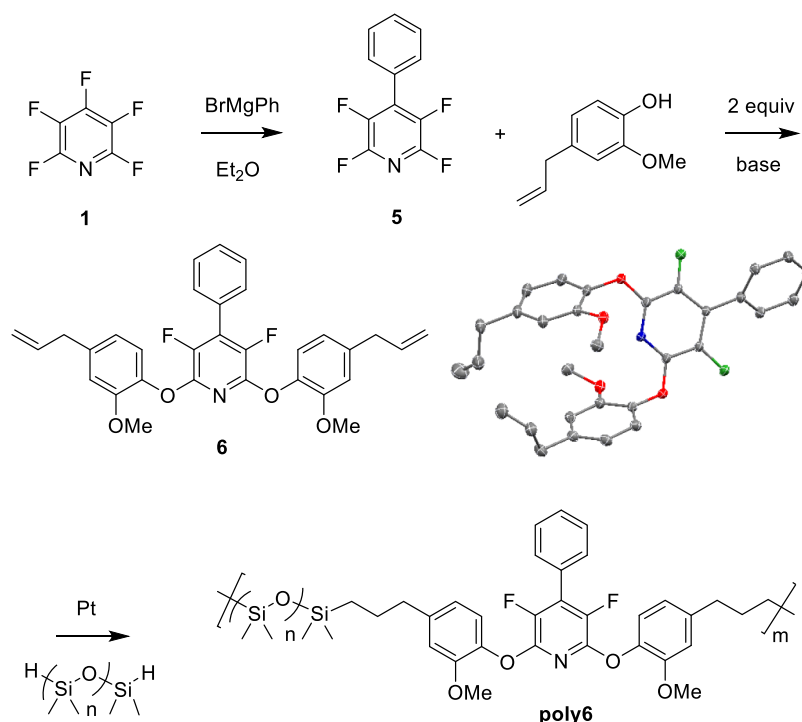
xylene) was added and the reaction allowed to stir at room temperature until gelation of the sample. The sample was then placed in a vacuum oven and the elastomers were cured at 200 °C for 48 h. The elastomers were purified by Soxhlet extraction with refluxing toluene for 16 h. The purified materials were dried in a vacuum oven at 60 °C prior to thermal characterization.

General Synthesis of Networks net9 and net10. To compound 7 or 8 (0.375 mmol) was added hydride terminated octasilane $Q_8M_8^H$ (1.0 mmol) in a minimal amount of toluene, enough to promote dissolution. The vial was then vortexed at room temperature for 1 min; 1 drop of Pt catalyst (5 wt % platinum divinyltetramethyldisiloxane complex in xylene) was added and the reaction allowed to stir at room temperature until gelation of the sample. The sample was then placed in a vacuum oven and were cured at 200 °C for 48 h. The network samples were purified by Soxhlet extraction with refluxing methanol for 16 h. The purified materials were dried in a vacuum oven at 60 °C prior to thermal characterization, whereby >95% of dried mass was recovered.

RESULTS AND DISCUSSION

Fluoropyridine siloxane-functionalized linear polymer systems were initially prepared by synthesizing the difunctional pentenyl ether-derivatized 3,5,6-fluoropyridine monomer (2) in multi-gram quantities from commercial FFP (1) by controlled addition of 4-penten-1-ol, under mild carbonate base conditions in excellent isolated yield (86%), as shown in Scheme 2. 4-Bromophenol can be conveniently substituted on the 6-position of monomer 2 under mild carbonate conditions to afford the 3,5-fluoropyridine monomer 3, which demonstrates the utility of pre-installing latent-reactive functionalities on the monomeric unit. We have reported on expansive examples of nucleophile additions to polymers poly2 and poly3 prepared from monomers 2 and 3, respectively, by mild Pt-catalyzed hydrosilylation with H-PDMS with a number-average molecular weight (M_n) of 1000 g mol⁻¹ ($n \sim 13$). ¹H NMR confirmed the quantitative conversion of the AMX

Scheme 4. Synthesis of Dieugenol Monomer 6 with ORTEP Projection with Atomic Displacement Ellipsoids Shown at the 50% Probability Level and Subsequent Polymerization with H-PDMS to poly6



pattern of the terminal alkenes with broad multiplets at 5.90–5.80 ppm ($CH=$) and 5.05–4.90 ppm ($CH_2=$) to 1.50–1.45 ($-CH_2-$) ppm and 0.58–0.54 ($-\text{Si}(\text{CH}_3)_2\text{CH}_2-$). The integration ratio of PDMS ($-\text{Si}(\text{CH}_3)_2-$), whereby $n = 13$, with the affixed aliphatic pentyl chain confirmed 13:1 integration of the represented repeat structure shown in Scheme 2 and ^1H NMR spectra in the Supporting Information. Furthermore, ^{19}F NMR proved a useful diagnostic tool to validate the post-functionalization, whereby only the -93.7 ppm shift from the F in the 6-position is present in 2 and the shifts -161.1 and -163.1 ppm are retained due to the desymmetrized F's in the 3,5-positions of 3 with no indication of polymer degradation. The ^{19}F NMR of the subsequent polymers **poly2** and **poly3** demonstrated similar patterns to those of the monomers with the presence of the multiple, broadened peaks, representative of polymer backbone dispersity. In only the case of **poly3**, incomplete conversion (less than 12%) of the terminal alkenes was observed by ^{19}F NMR, possibly due to the steric encumbrance of the bulky 1,4-arylbromoether moiety promoting polymer chain entanglement.

In order to expand the scope of linear perfluoropyridine (PFP)-based silicone polymers, aromatic functionalities were introduced using eugenol, a naturally sourced feedstock from clove oil, which possesses orthogonal reactivity as a nucleophile (via phenol) and an electrophilic terminal alkene. The addition of two equivalents of eugenol resulted in the formation of monomer 4, in a non-optimized yield of 34% due to the competitive tri-substituted addition of eugenol, which was mimicked to afford a similar strategy in the preparation of **poly2** and **poly3** to demonstrate post-functionalization (Scheme 3). Although the polymerization of 4 with H-PDMS (M_n of 1000 g mol^{-1} , $n \sim 13$) resulted conclusively with the formation of fluorosilicone **poly4** as evidenced by ^1H and ^{19}F NMR, the ability to prepare the exclusive pre-installed

monomer 4 with phenol (**1a**) resulted in a mixture of products with competitive formation of primarily **1b**, as discovered by ^{19}F NMR analysis. These observations are consistent with previous reports whereby reaction equilibria exist between fluoride and aromatic O-nucleophiles when substituted at the 4-position (as comparably facile leaving groups), resulting in scrambling of the 2,4,6-position on the pyridine ring.²⁹

Because monomer 4 caused scrambling at the 6-position, phenyl magnesium bromide addition to 1 as a C-nucleophile in the 4-position afforded intermediate 5, whereby no competitive equilibrium exists with fluoride in the 2,6-positions, as illustrated in Scheme 4. Therefore, monomer 6 was prepared in good isolated yield (77%) as an alternative route. Polymerization of 6 with H-PDMS (M_n of 1000 g mol^{-1} , $n \sim 13$) afforded fluorosilicone **poly6** as characterized by ^1H and ^{19}F NMR. Although this route does not provide for post-functionalization, the ability to pre-install substituents of interest in the 4-position via C-nucleophile addition from Grignard or lithiated intermediates demonstrates the potential for an expanded polymer pool with functionalized pendant groups.

The linear polymers prepared in this study produced acceptable number-average molecular weights (M_n) with molar mass dispersity indexes (\mathcal{D}) of 2.20–3.55, as determined by GPC, which is typical of step-growth polymerizations under optimized, Pt-catalyzed conditions, affording viscous oils (Table 1). From the GPC data, **poly2** and **poly4** had similar M_n values of $7000\text{--}8700\text{ g mol}^{-1}$, whereby functionalized polymers **poly3** and **poly6** exhibited a higher M_n , $12,700\text{--}13,200\text{ g mol}^{-1}$, presumably due to larger hydrodynamic volume due to the presence of the additional pendant aryl groups. Thermal analysis using DSC showed consistent, narrow T_g 's in the range of -28 to $-25\text{ }^\circ\text{C}$ for **poly2**, **poly4**, and **poly6**. The bulkiness of the 4-bromophenol side-chain-functionalized polymer **poly3** showed an expected

Table 1. Selected Properties of Linear Polymers

entry	$M_n \times 10^{-3}$ GPC ^a	D^a	T_g (°C) ^b	T_d (°C) ^c	char yield (%)
poly2	7.00	2.20	-25	360	3
poly3 ^d	12.7	2.50	-12	404	2
poly4	8.70	3.51	-26	388	14
poly6	13.2	2.89	-28	382	13

^aGPC in tetrahydrofuran using polystyrene as the standard. ^bDSC (5 °C min⁻¹) in nitrogen determined by the third heating cycle. ^cTGA onset (10 °C min⁻¹) of chain-extended polymers in argon. ^dFrom monomer 3 and post-modification of poly2 afforded the same values within error and were reported as the average of the two.

marked increase in T_g of -12 °C, compared with the non-functionalized poly2 analogue. TGA showed all polymers possessing an onset of thermal decomposition (T_d) at >360 °C in nitrogen, with the highest exhibited from the more thermally stabilized aryl bromo-functionalized polymer, poly3. TGA also produced char yields of 2–3% in nitrogen for the predominately aliphatic polymers poly2 and poly3, whereby higher aromatic content polymers poly4 and poly6 afforded expected increased char yields of 13–14%.

By derivatizing PFP at the 2,4,6-positions with 4-pentene-1-ol and eugenol under mild basic conditions, tri-functionalized monomers 7 and 8 were prepared, respectively (Scheme 5). The synthesis of 7 and 8 has been previously reported and were used for the preparation of elastomeric binders possessing programmable thermal properties via thiol-ene chemistry.³² An expansion of this work herein demonstrates the ability to prepare networked siloxane-based elastomers, whereby the H-PDMS units are introduced at varying molecular weights from commercially available sources, with repeat units of $n = 1, 5, 60,$ and 230 . To promote highly densified cross-linked elastomers, either monomer 7 or 8 was cured with the desired H-PDMS at 200 °C for 48 h and, upon Soxhlet extraction with toluene, afforded tough, rubbery solids that only swelled in refluxing toluene or dimethylsulfoxide at room temperature.

Selected thermal properties of networked 3,5-fluoropyridine functionalized silicone elastomers net7 and net8 using DSC and TGA are illustrated in Table 2. The pentyl ether

functionalized network series net7a–7d demonstrated slight improvement in thermal stability with post-Soxhlet extraction compared with no extraction presumably due to the removal of the residual Pt catalyst that is known to cause accelerated thermal degradation with T_d exceeding 378 °C to as high as 418 °C with increasing PDMS chain-length (n) inclusion.⁹ A similar trend is observed of higher char yield with increasing PDMS chain length up to 43% for net7c that possesses higher silicon content, which oxidizes to SiC and SiO₂ char under inert polymer pyrolysis of the post-Soxhlet sample. Surprisingly, the T_g remains relatively unaffected, ranging -42 to -49 °C by chain length for net7a and net7b, whereby longer chain length is expected to induce a plasticizing effect and increasing network chain mobility, thus lowering T_g . These results indicate that networks net7a and net7b are highly densified from both chemical and physical cross-linking from mobile aliphatic ether linkages with PDMS. Only a slight decrease in T_g and a pronounced melt transition (T_m) is observed for net7c and net7d at -46 and -38 °C, respectively, due to an onset of plasticizing and/or higher polydispersity present in the H-PDMS with extended siloxanes ($n = 60$ to 230), inducing bulk crystalline morphology in the confined network.

Monomer 8 networked with H-PDMS afforded thermally cross-linked species net8a–8d with mixed results. It is clear overall that the bulky eugenol units in the cross-linked framework complicated cure kinetics and ultimately thermal properties. Attempts to cure 8 with H-PDMS ($n = 1$) failed to produce the intractable rubbery elastic solid, net8a, even with increased Pt catalyst loading. However, highly densified networks net8b–8d were successfully prepared, possessing slightly higher T_d compared with the analogous net7b–7d series due to increasing aromatic content. Char yields ranged 25–34% but with no clear trend with increasing repeat units of H-PDMS. Curiously, net7b and net8b (both reacted with H-PDMS, $n = 5$) showed a significant increase in char yield with post-Soxhlet networks, which may be due to unbound H-PDMS due to the formation of cyclic structures. Finally, the T_g produced consistent results, whereby the highest was observed for net8b at 10 °C; net8c did not produce an observable T_g and net8d afforded -38 °C T_m inflection with increasing

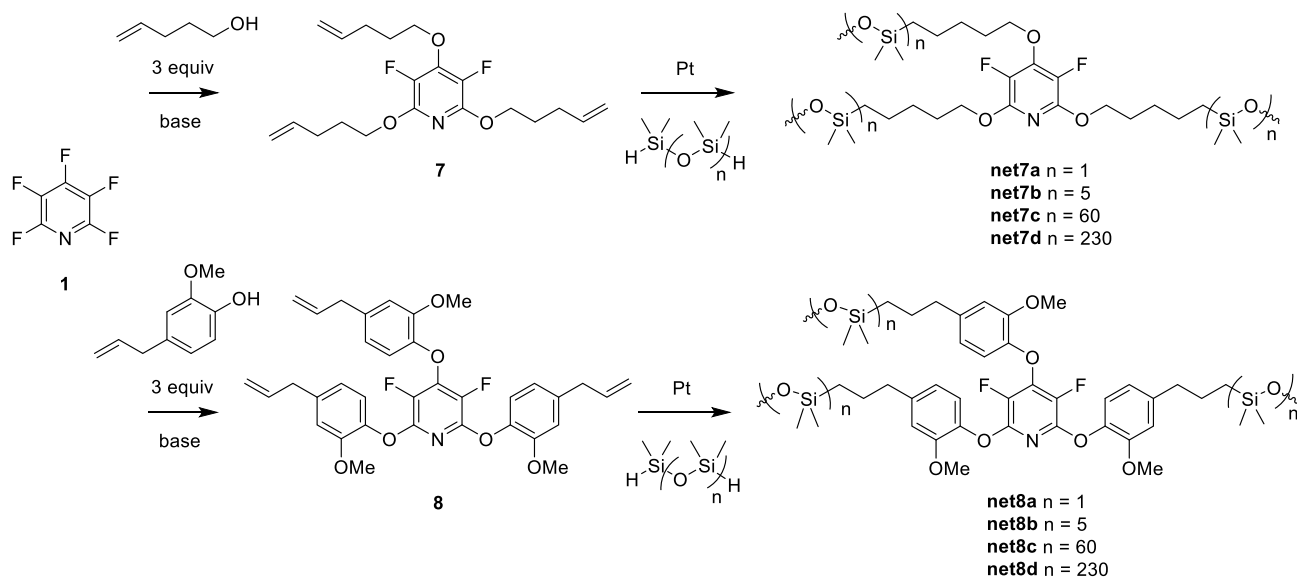
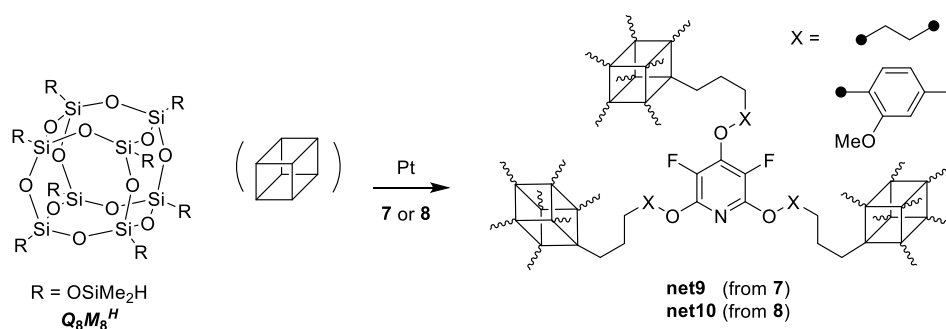
Scheme 5. Preparation of Network Polymers Monomer 7 and 8 with H-PDMS to Afford net7a–7d and net8a–8d, Respectively

Table 2. Selected Thermal Properties of Networks net7a–7d and net8a–8d

entry	H-PDMS repeat unit (<i>n</i>)	T_g^a pre-sox (°C)	T_g^a post-sox (°C)	T_d^b pre-sox (°C)	T_d^b post-sox (°C)	char yield pre-sox (%)	char yield post-sox (%)
net7a	1	−45	−45	377	378	9	9
net7b	5	−44	−43	380	379	4	18
net7c	60	−50	−49	400	409	42	43
net7d	230	^c	^c	410	418	36	33
net8a	1						
net8b	5	11	10	406	402	16	34
net8c	60			414	409	18	25
net8d	230	^d	^d	425	431	34	30
net9			28		407		49
net10			83		410		62

^aDSC (5 °C min^{−1}) in nitrogen determined by the third heating cycle. ^bTGA onset (10 °C min^{−1}) of chain-extended polymers in nitrogen. ^cMelt transition observed at −46 °C. ^dMelt transition observed at −38 °C.

Scheme 6. Cross-linking of $Q_8M_8^H$ with Either 7 or 8, Affording High Ceramic Char Upon Pyrolysis



PMDS units of $n = 230$, forming crystalline domains within the cross-linked matrix.

The comprehensive thermal study of networks **net7a–7d** and **net8a–8d** led to the utilization of octadimethyl cubic M_8Q_8 silane ($Q_8M_8^H$), commercially sourced as octasilane polyhedral oligomeric silsesquioxane (OctaSilane POSS) as the cross-linking agent possessing eight sites of functionality (Scheme 6). The additional sites of cross-linking afforded significantly more dense networks using stoichiometric equivalents as attributed by the higher T_g 's observed from the formation of **net9** ($Q_8M_8^H$ and 7) and **net10** ($Q_8M_8^H$ and 8) of 28 and 83 °C, respectively (see also Table 2). Although thermal stability (T_d) was comparable to that of **net7a–7d** and **net8b–8d**, the recorded char yields at 900 °C were significantly higher at 49 and 62%, respectively, as attributed to the Si–O ceramic cage thermal stability under an inert atmosphere.

CONCLUSIONS

This work prepares both linear and network fluoropyridine-based siloxane polymers by utilizing the unique regioselectivity of PFP to prepare monomers with varying degrees of functionalization by programming nucleophiles (O-nucleophiles in addition to possibly C-, N-, S-, or P-nucleophiles) at the 2,4,6-positions. Furthermore, the ability to pre-install or post-functionalize moieties of interest by substitution of the 6-position of difunctionalized aryl/alkyl ether monomers or their subsequent polymers affords expanded utility of these polymeric systems. Although this study demonstrates the general utility of monomer synthesis and subsequent polymerization, one can conceive the application of using additional main-group nucleophiles of interest such as C-, N-, P-, S-nucleophiles, given the facile

electrophilic nature of PFP which is relatively unexplored. In addition, the ability to decorate PFP with aliphatic/aromatic and/or a combination of nucleophiles possessing latent reactivity could provide access to tunable thermal, rheological, electrical, and surface energy properties that warrant further exploration for a myriad of material applications.

ASSOCIATED CONTENT

Supporting Information

The Supporting Information is available free of charge at <https://pubs.acs.org/doi/10.1021/acs.macromol.1c00333>.

NMR spectra and single crystal X-ray diffraction methods for elucidation of **6** (PDF)

AUTHOR INFORMATION

Corresponding Authors

Abby R. Jennings – Department of Chemistry & Chemistry Research Center, Laboratories for Advanced Materials, United States Air Force Academy, Colorado Springs 80840-6226, Colorado, United States; Email: abby.jennings@usafa.edu

Scott T. Iacono – Department of Chemistry & Chemistry Research Center, Laboratories for Advanced Materials, United States Air Force Academy, Colorado Springs 80840-6226, Colorado, United States; orcid.org/0000-0002-2313-2618; Email: scott.iacono@usafa.edu

Authors

Kevin A. Stewart – Department of Chemistry & Chemistry Research Center, Laboratories for Advanced Materials, United States Air Force Academy, Colorado Springs 80840-6226, Colorado, United States

Dylan Shuster – Department of Chemistry & Chemistry Research Center, Laboratories for Advanced Materials, United States Air Force Academy, Colorado Springs 80840-6226, Colorado, United States

Maria Leising – Department of Chemistry & Chemistry Research Center, Laboratories for Advanced Materials, United States Air Force Academy, Colorado Springs 80840-6226, Colorado, United States

Isaac Coolidge – Department of Chemistry & Chemistry Research Center, Laboratories for Advanced Materials, United States Air Force Academy, Colorado Springs 80840-6226, Colorado, United States

Erica Lee – Department of Chemistry & Chemistry Research Center, Laboratories for Advanced Materials, United States Air Force Academy, Colorado Springs 80840-6226, Colorado, United States

Charles Stevens – Department of Chemistry & Chemistry Research Center, Laboratories for Advanced Materials, United States Air Force Academy, Colorado Springs 80840-6226, Colorado, United States

Andrew J. Peloquin – Department of Chemistry & Chemistry Research Center, Laboratories for Advanced Materials, United States Air Force Academy, Colorado Springs 80840-6226, Colorado, United States

Daniel Kure – Department of Chemistry & Chemistry Research Center, Laboratories for Advanced Materials, United States Air Force Academy, Colorado Springs 80840-6226, Colorado, United States

Complete contact information is available at:

<https://pubs.acs.org/10.1021/acs.macromol.1c00333>

Notes

The authors declare no competing financial interest.

ACKNOWLEDGMENTS

The authors acknowledge financial support from the Defense Threat Reduction Agency (DTRA) and the Air Force Office of Scientific Research (AFOSR).

REFERENCES

- (1) Falzon, B. G.; Pierce, R. S. Thermosetting Composite Materials in Aerostructures. In *Revolutionizing Aircraft Materials and Processes*; Pantelakis, S., Tserpes, K., Eds.; Springer International Publishing: Cham, 2020; pp 57–86.
- (2) George, K.; Panda, B. P.; Mohanty, S.; Nayak, S. K. Recent Developments in Elastomeric Heat Shielding Materials for Solid Rocket Motor Casing Application for Future Perspective. *Polym. Adv. Technol.* **2018**, *29*, 8–21.
- (3) Zhang, R.; Pinhas, A. R.; Mark, J. E. Synthesis of Poly-(Tetramethyl-m-Silphenylenesiloxane), an Elastomer of Enhanced High-Temperature Stability. *Macromolecules* **1997**, *30*, 2513–2515.
- (4) Weinhold, F.; West, R. The Nature of the Silicon-Oxygen Bond. *Organometallics* **2011**, *30*, 5815–5824.
- (5) Gonzaga, F.; Yu, G.; Brook, M. A. Polysiloxane Elastomers via Room Temperature, Metal-Free Click Chemistry. *Macromolecules* **2009**, *42*, 9220–9224.
- (6) Rambarran, T.; Gonzaga, F.; Brook, M. A. Generic, Metal-Free Cross-Linking and Modification of Silicone Elastomers Using Click Ligation. *Macromolecules* **2012**, *45*, 2276–2285.
- (7) Yang, H.; Liu, M.-X.; Yao, Y.-W.; Tao, P.-Y.; Lin, B.-P.; Keller, P.; Zhang, X.-Q.; Sun, Y.; Guo, L.-X. Polysiloxane-Based Liquid Crystalline Polymers and Elastomers Prepared by Thiol-Ene Chemistry. *Macromolecules* **2013**, *46*, 3406–3416.

(8) Zhu, C.; Yang, H.; Liang, H.; Wang, Z.; Dong, J.; Xiong, L.; Zhou, J.; Ke, J.; Xu, X.; Xi, W. A Novel Synthetic UV-Curable Fluorinated Siloxane Resin for Low Surface Energy Coating. *Polymers* **2018**, *10*, 979.

(9) Jennings, A. R.; Morey, A. M.; Guenther, A. J.; Iacono, S. T. Synthesis and Characterization of Siloxane-Based Cyanate Ester Elastomers from Readily Available Materials: A Top-down Approach. *Polym. Int.* **2017**, *66*, 540–547.

(10) Hamdani, S.; Longuet, C.; Perrin, D.; Lopez-cuesta, J.-M.; Ganachaud, F. Flame Retardancy of Silicone-Based Materials. *Polym. Degrad. Stab.* **2009**, *94*, 465–495.

(11) Doede, C.; Panagrossi, A. Polysiloxane Elastomers. *Ind. Eng. Chem.* **1947**, *39*, 1372–1375.

(12) Oglioni, E.; Yu, L.; Mazurek, P.; Skov, A. L. Designing Reliable Silicone Elastomers for High-Temperature Applications. *Polym. Degrad. Stab.* **2018**, *157*, 175–180.

(13) Scott, D. W. Thermal Rearrangement of Branched-Chain Methylpolysiloxanes. *J. Am. Chem. Soc.* **1946**, *68*, 356–358.

(14) Tong, C.; Tian, Z.; Chen, C.; Li, Z.; Modzelewski, T.; Allcock, H. R. Synthesis and Characterization of Trifluoroethoxy Polyphosphazenes Containing Polyhedral Oligomeric Silsesquioxane (POSS) Side Groups. *Macromolecules* **2016**, *49*, 1313–1320.

(15) Lichtenhan, J. D.; Pielichowski, K.; Blanco, I. POSS-Based Polymers. *Polymers* **2019**, *11*, 1727.

(16) Lichtenhan, J. D.; Vu, N. Q.; Carter, J. A.; Gilman, J. W.; Feher, F. J. Silsesquioxane-Siloxane Copolymers from Polyhedral Silsesquioxanes. *Macromolecules* **1993**, *26*, 2141–2142.

(17) Liu, H.; Zheng, S. Polyurethane Networks Nanoreinforced by Polyhedral Oligomeric Silsesquioxane. *Macromol. Rapid Commun.* **2005**, *26*, 196–200.

(18) McMullin, E.; Rebar, H. T.; Mather, P. T. Biodegradable Thermoplastic Elastomers Incorporating POSS: Synthesis, Microstructure, and Mechanical Properties. *Macromolecules* **2016**, *49*, 3769–3779.

(19) Lee, K. M.; Knight, P. T.; Chung, T.; Mather, P. T. Polycaprolactone-POSS Chemical/Physical Double Networks. *Macromolecules* **2008**, *41*, 4730–4738.

(20) Yang, H.; He, C.; Russell, T. P.; Wang, D. Epoxy-Polyhedral Oligomeric Silsesquioxanes (POSS) Nanocomposite Vitrimers with High Strength, Toughness, and Efficient Relaxation. *Giant* **2020**, *4*, 100035.

(21) Hajjali, F.; Tajbakhsh, S.; Marić, M. Thermally Reprocessable Bio-Based Polymethacrylate Vitrimers and Nanocomposites. *Polymer* **2021**, *212*, 123126.

(22) Liu, Y.; Zhu, D.; Sun, J.; Li, J.; Wu, Y.; Gao, C. Synthesis and Characterization of a Novel Fluorosilicone Resin Based on Trifluoropropylalkoxysilane. *Mater. Chem. Phys.* **2019**, *224*, 40–46.

(23) Yan, Z.; Liu, W.; Wang, H.; Su, K.; Xia-Hou, G. Synthesis and Characterization of Novel Fluorinated Siloxane Star-like Copolymer with Short Perfluoroalkyl Chain and Used for Modification of the Epoxy Resin. *J. Fluorine Chem.* **2014**, *157*, 63–72.

(24) Tang, C.; Liu, W.; Ma, S.; Wang, Z.; Hu, C. Synthesis of UV-Curable Polysiloxanes Containing Methacryloxy/Fluorinated Side Groups and the Performances of Their Cured Composite Coatings. *Prog. Org. Coat.* **2010**, *69*, 359–365.

(25) Park, N. H.; Dos Passos Gomes, G.; Fevre, M.; Jones, G. O.; Alabugin, I. V.; Hedrick, J. L. Organocatalyzed Synthesis of Fluorinated Poly(Aryl Thioethers). *Nat. Commun.* **2017**, *8*, 1553.

(26) Dutta, T.; Woody, K. B.; Watson, M. D. Transition-Metal-Free Synthesis of Poly(Phenylene Ethynylene)s with Alternating Aryl-Perfluoroaryl Units. *J. Am. Chem. Soc.* **2008**, *130*, 452–453.

(27) Ding, J.; Qi, Y. The Preparation and Characterization of Highly Fluorinated Poly(Arylene Alkylene Ether)s. *Macromolecules* **2008**, *41*, 751–757.

(28) Gimenez, D.; Dose, A.; Robson, N. L.; Sandford, G.; Cobb, S. L.; Coxon, C. R. 2,2,2-Trifluoroethanol as a Solvent to Control Nucleophilic Peptide Arylation. *Org. Biomol. Chem.* **2017**, *15*, 4081–4085.

(29) Fuhrer, T. J.; Houck, M.; Corley, C. A.; Iacono, S. T. Theoretical Explanation of Reaction Site Selectivity in the Addition of a Phenoxy Group to Perfluoropyridine. *J. Phys. Chem. A* **2019**, *123*, 9450–9455.

(30) Corley, C. A.; Kobra, K.; Peloquin, A. J.; Salmon, K.; Gumireddy, L.; Knoerzer, T. A.; McMillen, C. D.; Pennington, W. T.; Schoffstall, A. M.; Iacono, S. T. Utilizing the Regioselectivity of Perfluoropyridine towards the Preparation of Phenoxyacetylene Precursors for Partially Fluorinated Polymers of Diverse Architecture. *J. Fluorine Chem.* **2019**, *228*, 109409.

(31) Peloquin, A. J.; Houck, M. B.; McMillen, C. D.; Iacono, S. T.; Pennington, W. T. Perfluoropyridine as an Efficient, Tunable Scaffold for Bis(Pyrazol-1-Yl)Pyridine Copper Complexes. *Eur. J. Inorg. Chem.* **2020**, *2020*, 1720–1727.

(32) Moore, L. M. J.; Greeson, K. T.; Stewart, K. A.; Kure, D. A.; Corley, C. A.; Jennings, A. R.; Iacono, S. T.; Ghiassi, K. B. Perfluoropyridine as a Scaffold for Semifluorinated Thiol-Ene Networks with Readily Tunable Thermal Properties. *Macromol. Chem. Phys.* **2020**, *221*, 2000100.

(33) Houck, M. B.; Brown, L. C.; Lambeth, R. H.; Iacono, S. T. Exploiting the Site Selectivity of Perfluoropyridine for Facile Access to Densified Polyarylene Networks for Carbon-Rich Materials. *ACS Macro Lett.* **2020**, *9*, 964–968.

(34) Eismeier, S.; Peloquin, A. J.; Stewart, K. A.; Corley, C. A.; Iacono, S. T. Pyridine-Functionalized Linear and Network Step-Growth Fluoropolymers. *J. Fluorine Chem.* **2020**, *238*, 109631.